

Effect of Irisin on trabecular bone in a streptozotocin-induced animal model of type 1 diabetic osteopathy; a micro-CT study

Sahar Mohsin ^{Corresp.,1}, Fiona Brock ², Suneesh Kaimala ¹, Charlene Greenwood ³, Mohsin Sulaiman ¹, Keith Rogers ², Ernest Adeghate ¹

¹ Department of Anatomy, College of Medicine and Health Sciences, United Arab Emirates University, Al Ain, Abudhabi, United Arab Emirates

² Cranfield Forensic Institute, Cranfield University, Shrivensham, United Kingdom

³ School of Chemical and Physical Sciences, Keele University, Newcastle-under-Lyme, Staffordshire, United Kingdom

Corresponding Author: Sahar Mohsin

Email address: smohsin@uaeu.ac.ae

Background. Osteoporosis is a significant co-morbidity of type 1 diabetes mellitus (DM1) leading to increased fracture risk. Exercise-induced hormone 'irisin' in low dosage has been shown to have a beneficial effect on bone metabolism by increasing osteoblast differentiation and reducing osteoclast maturation, and inhibiting apoptosis and inflammation. We investigated the role of irisin in treating diabetic osteopathy by observing its effect on trabecular bone. **Methods.** DM1 was induced by intraperitoneal injection of streptozotocin 60 mg/kg body weight. Irisin in low dosage (5 µg twice a week for 6 weeks I/P) was injected into half of the control and 4-week diabetic male Wistar rats. Animals were sacrificed six months after induction of diabetes. The trabecular bone in the femoral head and neck was analyzed using a micro-CT technique. Bone turnover markers were measured using ELISA, Western blot, and RT-PCR techniques. **Results.** It was found that DM1 deteriorates the trabecular bone microstructure by increasing trabecular separation (Tb-Sp) and decreasing trabecular thickness (Tb-Th), bone volume fraction (BV/TV), and bone mineral density (BMD). Irisin treatment positively affects bone quality by increasing trabecular number $p < 0.05$ and improves the BMD, Tb-Sp, and BV/TV by 21-28%. The deterioration in bone microarchitecture is mainly attributed to decreased bone formation observed as low osteocalcin and high sclerostin levels in diabetic bone samples $p < 0.001$. The irisin treatment significantly suppressed the serum and bone sclerostin levels $p < 0.001$, increased the serum CTX1 levels $p < 0.05$, and also showed non-significant improvement in osteocalcin levels. **Conclusions.** This is the first pilot study to our knowledge that shows that a low dose of irisin marginally improves the trabecular bone in DM and is an effective peptide in reducing sclerostin levels.

1 **Effect of Irisin on trabecular bone in a streptozotocin-**
2 **induced animal model of type 1 diabetic osteopathy; a**
3 **micro-CT study**

4

5 Sahar Mohsin¹, Fiona Brock ², Suneesh Kaimala ¹, Charlene Greenwood ³, Mohsin Sulaiman ¹,
6 Keith Rogers², Ernest Adeghate¹

7

8 ¹ Department of Anatomy, College of Medicine and Health Sciences, United Arab Emirates
9 University, Al Ain, United Arab Emirates

10 ² Cranfield Forensic Institute, Cranfield University, Shrivenham, UK

11 ³ School of Chemical and Physical Sciences, Keele University, Staffordshire, UK.

12

13

14 Corresponding Author:

15 Sahar Mohsin ¹

16 Khalifa Bin Zayed Street, Tawam, Al Ain, Abu Dhabi, UAE, 15551

17 Email address: smohsin@uaeu.ac.ae

18

19

20

21

22

23

24

25

26

27

28

29

30

31

32

33

34

35

36

37

38

39

40 **Abstract**

41 **Background.** Osteoporosis is a significant co-morbidity of type 1 diabetes mellitus (DM1)
42 leading to increased fracture risk. Exercise-induced hormone 'irisin' in low dosage has been
43 shown to have a beneficial effect on bone metabolism by increasing osteoblast differentiation
44 and reducing osteoclast maturation, and inhibiting apoptosis and inflammation. We investigated
45 the role of irisin in treating diabetic osteopathy by observing its effect on trabecular bone.

46 **Methods.** DM1 was induced by intraperitoneal injection of streptozotocin 60 mg/kg body
47 weight. Irisin in low dosage (5 µg twice a week for 6 weeks I/P) was injected into half of the
48 control and 4-week diabetic male Wistar rats. Animals were sacrificed six months after induction
49 of diabetes. The trabecular bone in the femoral head and neck was analyzed using a micro-CT
50 technique. Bone turnover markers were measured using ELISA, Western blot, and RT-PCR
51 techniques.

52 **Results.** It was found that DM1 deteriorates the trabecular bone microstructure by increasing
53 trabecular separation (Tb-Sp) and decreasing trabecular thickness (Tb-Th), bone volume fraction
54 (BV/TV), and bone mineral density (BMD). Irisin treatment positively affects bone quality by
55 increasing trabecular number $p < 0.05$ and improves the BMD, Tb-Sp, and BV/TV by 21-28%.
56 The deterioration in bone microarchitecture is mainly attributed to decreased bone formation
57 observed as low osteocalcin and high sclerostin levels in diabetic bone samples $p < 0.001$. The
58 irisin treatment significantly suppressed the serum and bone sclerostin levels $p < 0.001$,
59 increased the serum CTX1 levels $p < 0.05$, and also showed non-significant improvement in
60 osteocalcin levels.

61 **Conclusions.** This is the first pilot study to our knowledge that shows that a low dose of irisin
62 marginally improves the trabecular bone in DM and is an effective peptide in reducing sclerostin
63 levels.

64

65

66

67

68

69

70

71

72

73

74

75

76

77

78

79

80

81

82 Introduction

83 Type 1 diabetes mellitus (DM1) is associated with increased skeletal fragility, due to a decrease in
84 both bone mineral density (BMD) and altered bone quality (Janghorbani et al. 2006; Janghorbani
85 et al. 2007; Lebiedz-Odrobina & Kay 2010; Napoli et al. 2017). Patients with DM1 are at greater
86 risk of fracture due to an increasing tendency to fall not only as a result of peripheral neuropathy,
87 poor vision, and stroke but also due to increased bone loss and/or altered bone matrix and strength
88 (Janghorbani et al. 2006; Mohsin et al. 2019a; Vestergaard 2007).

89 DM1 not only affects bone mineral density but also affects bone quality, including bone turnover,
90 microarchitecture, mineralization, microdamage, and bone mineral composition (Hough et al.
91 2016; Mohsin et al. 2019a; Saito et al. 2006). Animal studies have shown changes in the bone
92 tissue as early as four to eight weeks after the onset of DM1 (Mohsin et al. 2019a). An increased
93 number of apoptotic osteocytes were found in diabetic rat bones, which explains the imbalance of
94 the remodeling cycle in DM1. Low levels of serum markers for bone formation such as osteocalcin
95 and bone alkaline phosphatase and increased levels of advanced glycation end products (AGEs)
96 were found in the streptozotocin-induced model of DM1 rats (Hygum et al. 2019; Khan & Fraser
97 2015; Miyake et al. 2018). Reports on bone resorption in DM1 are particularly controversial, being
98 reported as unchanged, decreased, or increased in animal and human population studies (Gallacher
99 et al. 1993; Maggio et al. 2010; Motyl & McCabe 2009; Motyl et al. 2009). The major pathogenetic
100 mechanism involved in DM1-induced bone deficit is insulin deficiency, along with glucose
101 toxicity, marrow adiposity, inflammation, adipokine, and other metabolic alterations (Hough et al.
102 2016).

103 Regular exercise improves the quality of life through its beneficial effects on various systems in
104 the body. Exercise also increases bone and muscle strength and helps prevent bone loss (Benedetti
105 et al. 2018). In turn, increasing physical activity in children with diabetes as well as good
106 glycaemic control appears to provide some improvement in bone parameters (Colberg et al. 2016).
107 Irisin peptide expressed in the skeletal muscle and released after physical activity is reported to
108 increase bone tissue mass and strength (Boström et al. 2012; Colaianni et al. 2015; Khan & Fraser
109 2015). It can improve insulin resistance, lower blood glucose and promote weight loss. Studies
110 have shown that irisin also helps in cell proliferation and inhibits cell apoptosis (Liu et al. 2017).
111 The role of irisin in diabetes is still unclear due to contradictory findings (Mahgoub et al. 2018).
112 A recent study (Tentolouris et al. 2018) has shown that circulating irisin levels were lower in
113 subjects with DM1 in comparison with healthy-matched controls. The low circulating irisin levels
114 is associated with advanced glycation end products (AGEs) accumulation and vascular
115 complications in diabetic patients (Rana et al. 2017), and irisin has been reported to have potent
116 anti-inflammatory properties (Mazur-Bialy et al. 2017).

117 Browning of adipose tissue is reported with a higher irisin dose (3,500 $\mu\text{g} \cdot \text{kg}^{-1}$ per week) but this
118 effect was not seen with low-dose recombinant irisin (r-irisin) in young male mice (Colaianni et
119 al. 2015). More recently it has been shown that irisin in a low dose of 100 $\mu\text{g} \cdot \text{kg}^{-1}$ has anabolic

120 effects on bone tissue without browning of adipose tissue. Irisin in low dose modulated the skeletal
121 genes, *Opn* (osteopontin) and *Sost* (Sclerostin) (Colaïanni et al. 2015; Holmes 2015). Cortical bone
122 mass and strength were markedly increased in irisin-treated mice, compared with control mice
123 (Colaïanni et al. 2015). However, this beneficial effect was only seen in cortical bone and no
124 changes were observed in the trabecular compartment of bone in mice. A marked increase in
125 cortical bone mass was attributed to the suppression of sclerostin which inhibits bone formation
126 through the Wnt signaling pathway, and stimulation of ‘osteoblasts’ (bone-forming cells)
127 (Colaïanni et al. 2015). Moreover, it deters bone resorption by inhibiting osteoclast differentiation
128 (Ma et al. 2018). Due to these actions on bone, irisin is known to enhance the mechanical properties
129 of bone (Gallacher et al. 1993).

130 Trabecular bone quality is significantly lower in adults with DM1 (Shah et al. 2018) and to our
131 knowledge, the effect of a low dose of irisin on the trabecular bone in DM has not yet been
132 investigated. This pilot study aimed to investigate the role of a very low dose of irisin in
133 ameliorating bone fragility associated with DM, by examining its effect on bone turnover markers
134 and, trabecular bone microstructure using a non-destructive microcomputed tomography (micro-
135 CT) technique in a single high-dose streptozotocin-induced model of DM1.

136

137

138 **Materials & Methods**

139 **Animal Handling, Induction of Diabetes, and Irisin Treatment**

140 Forty healthy male Wistar rats weighing between, 270 and 300 g were obtained from the Animal
141 House Facility at United Arab Emirates University (UAEU). National Institute of Health (NIH)
142 guidelines for the care and use of laboratory animals were followed for all experiments and
143 procedures carried out in this study after being approved by the Animal Research Ethics
144 Committee of the College of Medicine and Health Sciences (CMHS), UAE University
145 ERA_2018_5833.

146 The animals were housed singly in cages under standard conditions with a 12 h alternating light
147 and dark cycle, at 22–24 °C and 50–60% humidity, and provided with free access to standard rat
148 chow and water ad libitum during the two weeks of acclimatization and for the experimental
149 period. All efforts were made to minimize animal suffering and to limit the number of animals
150 used (Mohsin et al. 2019a). No adverse event was recorded during the period of the experiment.

151

152 A single intraperitoneal (I/P) injection of streptozotocin [STZ, Santa Cruz (U-9889) 60 mg/kg
153 body weight] dissolved in a freshly prepared citrate buffer (0.1 M, pH 4.5) was given to 12
154 normal Wistar rats to induce experimental DM1 (Furman 2015). The control rats were injected
155 with equal volumes of the vehicle. Diabetic animals had mean random blood glucose levels of
156 more than 24 mmol/l (Supl Fig 1). Irisin was injected into the treatment groups at 5 µg twice a
157 week for 6 weeks I/P. The animals were euthanized by CO₂ overdose using commercially
158 supplied compressed CO₂ in cylinders fitted with Murex Saffire 300 Bar Argon/CO₂ Mixed Gas
159 Regulator Gauge by a vet and trained staff in the animal facility at CMHS.

160

161 (100% CO₂ was introduced to the chamber at a fill rate of 50% of the chamber volume per
162 minute) followed by thoracotomy, 6 months after the induction of diabetes (Figure 1).

163

164 Figure 1: A streptozotocin-induced rat model of type 1 diabetic osteopathy injected with a low
165 dose of irisin.

166

167 Blood and bones were collected for ELISA, PCR, western blotting, and imaging using micro-CT.

168 Only 24 animals were used for this pilot study keeping in mind the 3Rs principle to see the effect

169 of the low dose of irisin if any in treating diabetic osteopathy and the rest of the animals were

170 shared with other researchers in the institution for future studies on other systems. Power

171 calculations were not carried out as it was a pilot study to test the effect of a very small dose of

172 irisin on the trabecular bone that was not reported before in the literature.

173 The experimental animals were equally allocated to different groups at random for treatments

174 and all procedures.

175 a) Control+vehicle (Normal untreated NUT)

176 b) Control+irisin (Normal treated NT)

177 c) Diabetic+vehicle (Diabetic untreated DMUT)

178 d) Diabetic+irisin (Diabetic treated DMT).

179

180 They were further subdivided for micro-CT, and bone turnover marker analysis at the end of the

181 experimental period (n=3 to 5) for each analysis. PI and research assistant was aware of the

182 group allocation at different stages of the experiment.

183

184 **Data Acquisition Using Microcomputed Tomography**

185 The bone microarchitecture of the neck of the femur was examined non-invasively using a

186 micro-CT (n=3/Gp). The area of the Ward triangle (Bouxsein et al. 2010b; Courtney et al. 1995)

187 was scanned to detect any early changes in bone mineral density. Each specimen was scanned

188 using a Nikon Metrology XT H225 (X-Tek Systems Ltd, Tring, Hertfordshire, UK) cone-beam

189 μ CT scanner operated at 65 kV, and 63 μ A, with an exposure time of 1000 ms. The geometric

190 magnification produced a voxel dimension of ca. 23 μ m for all the specimens. The software was

191 set to optimize projections (typically 1571), with 2 frames collected per projection. Noise

192 reduction and beam hardening corrections were applied to the data.

193 To determine the trabecular bone microarchitecture in the femoral head and neck area, bone

194 volume fraction (bone volume/total volume, BV/TV, %), trabecular bone thickness (Tb-Th,

195 mm), trabecular bone separation (Tb-Sp, mm), and trabecular bone number (Tb-N, mm⁻¹), the

196 ratio of segmented bone surface to the total volume of the region of interest (BS/BV, mm⁻¹), and

197 bone mineral density (BMD, g cm⁻³) were measured using VG Studio Max 2.2 (Volume

198 Graphics GmbH, Heidelberg, Germany) software. All trabecular bone microarchitectural

199 measurements of the femoral head and neck area excluded the cortical bone as in the earlier

200

201 vTMD values were used to determine volumetric bone mineral density values (vBMD) according
202 to: $vBMD = vTMD \times BV/TV$. vTMD refers to the density measurement restricted to within the
203 volume of calcified bone tissue and excludes any surrounding soft tissue, whereas vBMD is the
204 combined density in a well-defined volume (Estell et al. 2020).

205 A standard BMD phantom (QRM-microCT-HA, QRM GmbH, Moehrendorf, Germany) was
206 used to quantify density within the micro-CT images. The phantom used consists of five
207 cylindrical inserts of known densities of calcium hydroxyapatite (Ca-HA), $Ca_{10}(PO_4)_6(OH)_2$.
208 Proprietary epoxy resin is uniformly filled as the base material. The BMD values of the
209 cylindrical inserts were 1.13 gcm^{-3} , 50, 200, 800, and 1200 mgcm^{-3} .

210

211

212 **Real-time PCR analysis and Western blots**

213 Real-time PCR analysis and western blots were carried out in three to four randomly selected
214 rats from each experimental group, to estimate the levels of SOST/sclerostin expression in bone
215 samples at both transcriptional and translational levels. Real-time PCR was carried out by
216 extracting RNA from tibiae by following the trizol method of RNA extraction (Kelly et al.
217 2014). The high-capacity cDNA reverse transcription kit (Applied Biosystems, 4368813) was
218 used to synthesize cDNA from the extracted RNA. Real-time PCR analysis was performed using
219 the TaqMan primers specific for SOST gene (Thermo Scientific, 4331182) detection and was
220 normalized to β -actin (Thermo Scientific, 4331182) expression levels.

221 For western blots, a total protein was extracted from bone samples using a standard protocol.
222 Briefly, bones were powdered in liquid nitrogen and extracted using 1X RIPA buffer containing
223 protease and phosphatase inhibitors. Following centrifugation, the supernatant was collected and
224 assayed by western blot analysis. $20\mu\text{g}$ proteins were separated in a 4-12% SDS-PAGE
225 (Genscript, M00654) and transferred to the PVDF (Polyvinylidene fluoride) blotting membrane.
226 Following blocking with 5% milk in TBST (Tris Buffered Saline with Tween), the membrane
227 was probed using a primary antibody against sclerostin (AF 1589, Mouse SOST/sclerostin
228 antibody, 1:1000 dilution in 5% milk in TBST) and Rabbit anti-goat IgG secondary antibody
229 (Peroxidase conjugated, Cat# A4174, Sigma Aldrich, 1:6000 in TBST). The blots were
230 developed, and the images were captured on an X-ray film. The sclerostin western blot band
231 intensities were normalized to the expression of GAPDH estimated by western blot analysis of
232 the same samples using mouse monoclonal antibody against GAPDH (Sc-32233, Santa Cruz
233 Biotechnology, 1:3000 in 5% milk in TBST) and goat anti-mouse HRP- conjugated secondary
234 antibody (ab205719, 1:5000 in TBST) and shown as relative SOST expression.

235

236 **Enzyme-linked Immunosorbent Assay**

237 ELISA was carried out to estimate the bone turnover markers osteocalcin and C-terminal
238 telopeptide (CTX1) levels in serum and bone samples in three to five randomly selected rats
239 from each experimental group using a readymade kit from Abbkine Scientific (Osteocalcin,
240 KTE1010153) and Cloud-Clone (CTX-1, CEA665Ra) respectively and following the standard

241 manufacturer's protocol. Briefly, 50 μ l of the samples (for bone lysates, approximately 600 μ g
242 protein) or standards were applied to 96 well microtiter plates pre-coated with the ELISA capture
243 antibody, mixed with 50 μ l of 1:100 diluted biotin-conjugated competitor and further incubated
244 for 1hr at 37°C. The plates were washed thrice with the wash solution, incubated for 30 minutes
245 with 100 μ l of 1:100 diluted streptavidin-HRP, and washed five times with the wash solution.
246 The plates were incubated with 90 μ l of HRP substrate in the dark at 37°C and the colorimetric
247 reaction was quenched using a stop solution. The absorbance of the plate was measured at 450
248 nm spectrophotometrically (Tecan Infinite M200 Pro).

249

250 **Statistical Analysis**

251 The data were analyzed using One-way or Two-way ANOVA with Turkey or Bonferroni post-
252 test multiple comparison tests using commercially available software GraphPad Prism 9.0.0 for
253 Windows, San Diego, California. Adjusted p-value (*p < 0:05, **p < 0:01). Data is presented as
254 mean \pm standard error (SE).

255

256 **Results**

257

258 **Trabecular bone morphometry using microcomputed tomography (micro-CT)**

259 Data for all the measured trabecular bone structural parameters is presented in Table 1 as mean \pm
260 SE while Figure 2 displays the 3D images of the micro-CT scans for each of the four
261 experimental groups along with the plots depicting changes in various structural parameters of
262 trabecular bone.

263

264 The untreated diabetic group (DMUT) demonstrated an increase in the mean distance between
265 trabeculae, resulting in larger marrow spaces (Table 1, Figure 2). The trabecular separation
266 showed a significant 59% increase between the control group NUT (mean \pm SE: 0.09867 \pm
267 0.007) and DMUT (mean \pm SE: 0.1570 \pm 0.008). Treatment with irisin reduced the trabecular
268 separation to 28% in the diabetic samples (mean \pm SE: 0.1137 \pm 0.008), although this change
269 was not statistically significant (p > 0.05).

270

271 In terms of trabecular count, DMUT (mean \pm SE: 4.243 \pm 0.24) had a lower value compared to
272 NUT (mean \pm SE: 4.910 \pm 0.082), although the difference was not statistically significant.

273 Treatment with irisin resulted in a significant increase (p < 0.05) in the number of trabeculae in
274 the diabetic samples (mean \pm SE: 5.222 \pm 0.268), with a recorded difference of 23%. Trabecular
275 thickness decreased by 23% in DMUT (mean \pm SE: 0.0803 \pm 0.008) compared to the control
276 NUT samples, and the irisin treatment did not show a significant improvement in this parameter
277 (DMT: mean \pm SE: 0.0789 \pm 0.0023).

278 DM had a negative impact on bone volume fraction (BV/TV), as evident in the comparison
279 between NUT, NT, and DMUT, with a significant decrease of 34.5% in DMUT compared to the
280 untreated controls (NUT). Notably, the irisin treatment led to a 21.7% improvement in bone

281 volume. Bone mineral density (BMD) exhibited a significant decrease in DM, with a statistically
 282 significant change of 39% calculated between the control NUT (mean \pm SE: 0.7527 ± 0.05921)
 283 and DMUT (mean \pm SE: 0.4580 ± 0.042) samples. The irisin treatment showed an increase of
 284 27% in BMD (mean \pm SE: 0.5820 ± 0.021) for the diabetic samples.

285

286 **Table 1:** Mean \pm S.E between different groups related to trabecular bone parameters obtained
 287 using micro-CT. normal un-treated/ NUT, normally treated (NT), diabetic un-treated (DMUT), and
 288 diabetic treated (DMT). Trabecular separation Tb-Sp (NUT-DMUT = $P < 0.05$: Trabecular
 289 thickness Tb-Th (NT-DMUT; NT-DMT = $P < 0.05$): Trabecular number Tb-N Gp (DMUT-DMT = P
 290 < 0.05): bone volume/total volume BV/TV Gp (NUT-DMUT; NT-DMUT = $P < 0.05$): bone surface
 291 density BS/ BV Gp (NT-DMUT; NT-DMT $P < 0.05$): Bone mineral density BMD Gp (NUT-DMUT;
 292 NT-DMUT = $P < 0.05$). n=3/Gp.

293

294

295 **Figure 2:** Representation of 3D microarchitecture of the trabecular bone at the proximal end of
 296 the femur is shown in frontal (A, C, E, and G) and cross-sectional (B, D, F, and H) images from
 297 four groups: A and B (Normal un-treated/ NUT), C & D (Normal treated / NT), E and F (diabetic
 298 un-treated / DMUT), and G & H (treated / DMT) obtained by using the micro-CT. The image I is
 299 the magnified image of (A) to show the region of interest for frontal (red box) and cross-sectional
 300 (blue line) images. Plots of changes in various structural parameters of trabecular bone n=3/Gp:
 301 (J) Trabecular separation (Tb-Sp) (K) Trabecular thickness (Tb-Th) (L) Trabecular number (Tb-
 302 N) (M) Bone volume/total volume BV/TV, (N) Bone surface density (BS/TV) (O) mean 1 (BMD),
 303 from NUT, NT, DMUT, DMT compared. P values are indicated in brackets.

304

305

306

307 **Effect of irisin on bone turnover markers**

308

309 Bone formation decreased significantly in diabetes as indicated by the decreased osteocalcin
 310 levels in sera and bone samples in DMUT (Figures 3A and 3B).

311

312

313 **Figure 3:** Plots of changes in bone markers in sera and bone tissue is shown (A-E) in all four
 314 groups (Normal un-treated NUT: Normal Treated NT: Diabetic untreated DMUT: Diabetic treated
 315 DMT) n= 3-5/Gp; F (n=3-4/Gp): (A) Serum osteocalcin (ng/ml) (B) Bone osteocalcin (pg/ml) (C)
 316 Serum CTX1 (ng/ml)(D) Bone CTX1 (pg/ml). Relative SOST expression is shown by PCR (E),
 317 Western blot (F). P values are indicated in brackets. Error bars = Mean \pm SE.

318

319 Irisin treatment has anabolic action and it improved the osteoblastic activity reflected in raised
 320 osteocalcin levels, although the change was not statistically significant. Bone resorption as
 321 indicated by measuring CTX-1 in serum and bone samples indicates that resorption increases
 322 significantly in diabetes. Treatment with irisin further increased osteoclastic activity and this

323 effect was significant in NT bone samples when compared with those of NUT (Figures 3C and
324 3D).

325

326 We also observed that SOST levels were increased significantly in DMUT compared to NUT
327 bone samples (Figure 3F) $p < 0.01$ and were significantly down-regulated with irisin treatment in
328 diabetic samples ($p < 0.01$) in both serum and bone samples (Figure 3E and 3F and Suppl data
329 1a, 1b)

330

331

332 Discussion

333 DM1 is associated with poor bone health and a 6-fold increase in the overall incidence of hip
334 fractures (Janghorbani et al. 2006; Janghorbani et al. 2007). Exercise improves many diabetic
335 complications (Colberg et al. 2016). Physical activity stimulates the production of PGC-1 α
336 (peroxisome proliferator-activated receptor- γ co-activator 1 α) in skeletal muscles, which in turn
337 leads to the synthesis of FNDC5 (fibronectin type III domain-containing protein 5), a membrane
338 protein abundantly found in skeletal muscles. Following exercise, there is an observed increase
339 in the levels of irisin peptide, which is derived from the cleavage of its precursor protein FNDC5,
340 as demonstrated in the research by Boström et al. in 2012.

341 The research conducted by Faienza et al. in 2018 revealed a significant inverse correlation
342 between levels of irisin and the duration of diabetes. Another study found that the circulating
343 irisin levels were lower in patients with diabetes when compared with healthy-matched controls
344 (Tentolouris et al. 2018). Colaianni et al. 2015 and Faienza et al. 2018 have shown that irisin is
345 directly involved in bone metabolism, by promoting the differentiation of bone marrow stromal
346 cells into mature osteoblasts. We specifically used a very small dose of irisin in this pilot study
347 that has not been previously reported for bone tissue research. This decision was based on
348 previous evidence showing that even a low dose of irisin, as low as 15 ng/ml, can increase
349 AMPK levels in cells. Additionally, it has been demonstrated that 15 ng/ml is the observed
350 serum level of irisin in diabetic rats after exercise (Formigari et al., 2022). Other studies have
351 utilized doses of 50 ng and 100 ng of irisin to effectively stimulate significant increases in
352 rodents (Kutlu et al., 2023). Furthermore, a recent study reported that irisin at a dose of 10 ng/ml
353 can inhibit cell death and prevent mineral loss in bone tissue (Cariati et al., 2023).

354 Our study investigated the effect of DM1 on trabecular bone microstructure in the proximal
355 femur obtained from mature male Wistar rats using a micro-CT. Furthermore, we examined the
356 potential therapeutic effects of irisin in mitigating type 1 diabetic osteopathy induced by STZ.
357 Additionally, the study evaluated changes in bone turnover markers after irisin treatment,
358 including those specifically related to DM1.

359 Wistar rats are commonly used in animal research due to similarities in pathophysiologic
360 responses between the human and rat skeleton, combined with the husbandry and financial
361 advantages (Lelovas et al. 2008). Micro-CT is the most powerful non-invasive technique that has
362 completely revolutionized the assessment of bone architecture *ex vivo*. It is considered a gold

363 standard technique for evaluating bone microstructure in small animal models. In a previous
364 study by Mohsin et al. in 2019b, we successfully utilized micro-CT to analyze bone
365 microarchitecture in type 2 diabetes, specifically focusing on the head and neck of the femur at a
366 high resolution without causing specimen damage. By acquiring X-ray attenuation data from
367 multiple angles, micro-CT reconstructs a detailed 3D representation of the specimen. The
368 scanning and data analyses adhered to established guidelines for assessing bone microstructure in
369 rodents, as outlined by Bouxsein et al. in 2010a.

370 In this study, the Ward area was also included in the trabecular and BMD measurements. Ward's
371 triangle is situated at the base of the femoral neck and is regarded as an area of minor resistance.
372 It is defined by the joining of trabeculae of varying lengths and widths depending on the
373 dimensions of the femoral neck which varies with age. The change in bone mineral density
374 occurs early at Ward's triangle; therefore, evaluation of bone mineral density in this area
375 contributes to an understanding of femoral neck bone mass distribution and any imbalance is
376 particularly important to assess the risk of bone fragility (Bouxsein et al. 2010b; Furman 2015).
377 DM adversely affects bone tissue making it porous and causing a decrease in bone volume/total
378 volume, an increase in bone turnover (BS/BV), and a significant decrease in BMD (Chen et al.
379 2018). However, a case-control study comparing the results of iliac biopsies taken from diabetic
380 subjects with those from healthy age- and sex-matched non-diabetic controls found no
381 differences in bone histomorphometric or micro-CT measurements (Armas et al. 2012).

382 Our study revealed several significant findings regarding the impact of diabetes on trabecular
383 bone microstructure. We observed a notable increase in the distance between adjacent trabeculae,
384 as indicated by increased trabecular separation (Tb-Sp), along with thinning of trabeculae in the
385 DMUT group. Furthermore, we found an elevated bone surface-to-bone volume ratio (BS/BV) in
386 the diabetic groups, suggesting increased osteoclast activity in diabetes. Although the number of
387 trabeculae decreased in the DMUT group compared to the NUT group, the decrease was not
388 statistically significant.

389 Bone volume fraction (BV/TV) is the percentage ratio of the mineralized bone volume to the
390 total volume of the region of interest in a sample is negatively affected by DM1 in this study.
391 Trabecular BV/TV is lower in patients who have sustained vertebral and hip fractures (Boutroy
392 et al. 2011; Ciarelli et al. 2000; Legrand et al. 2000; Milovanovic et al. 2012). The reduced
393 BV/TV is most likely due to decreases in Tb-N and increases in Tb-Sp which is often found in
394 age-related trabecular bone loss with or without thinning of trabeculae (McCalden et al. 1997;
395 Thomsen et al. 2002). The trabecular bone strength is dependent on the meshwork of intact
396 trabecular plates of normal width (Thomsen et al. 2002). Treatment with a low dose of irisin 5 μ g
397 twice a week for 6 weeks I/P increased the BV/TV by 21.7% in GP IV-DMT irisin-treated group
398 as compared with the saline-treated group DMUT. Tb-Sp also decreased (28%) in the DMT
399 however the treatment did not improve the Tb-Th or BS/BV in DMT. The number of trabeculae
400 significantly increased with irisin treatment DMT. It is most likely that irisin results in improved
401 BV/TV due to an increase in trabecular number and reduced trabecular separation. Reduction in
402 BV/TV is a key structural alteration observed in osteoporotic bone, and it has been correlated

403 with overall bone strength in various studies, including those conducted by Riggs & Parfitt in
404 2005, Thomsen et al. in 1998, and Zhang et al. in 2010.

405 A measure of bone mineral density (BMD, mg cm^{-3}) is important in the evaluation of
406 osteoporosis and other bone-related conditions. Low bone mineral density along with poor bone
407 quality is a risk factor for fragility fractures (Ciarelli et al. 2000; Marshall et al. 1996; Siris et al.
408 2001; Zhang et al. 2010). In this study, we observed that BMD significantly decreased in the
409 untreated diabetic group of animals and irisin treatment improved the bone mineral density by
410 27%.

411 This study did not find a statistically significant change in the trabecular bone parameters in
412 irisin-treated healthy animals in the control group. This is in agreement with a previously
413 published study (Colaianni et al. 2015) which found no change in trabecular bone morphology
414 related to Tb. Th, Tb-N, and Tb-Sp in mice treated with a low dose of r-irisin compared with the
415 control mice. However, that study reported increased cortical bone mineral density and a positive
416 effect on cortical bone geometry following irisin treatment (Colaianni et al. 2015). Nevertheless,
417 a recent study of micro-CT analysis of femurs (Colaianni et al. 2017) showed that r-irisin
418 maintained bone mineral density in both cortical and trabecular bone, and prevented a significant
419 decrease of the trabecular bone volume fraction in hind-limb suspended mice. The thickening of
420 the cortical bones after the irisin treatment is also evident in our experiments (Figures 2D and
421 2H).

422 The alteration in the bone microstructure is attributed to changes in the remodeling cycle.
423 Homeostasis in bone requires a balance between bone formation and resorption. Proper
424 vascularisation is indispensable to maintain homeostasis. The impairment of blood supply to the
425 bone tissue as occurs in diabetes could change the proliferation and differentiation of bone
426 precursors in the bone marrow resulting in an altered bone remodeling cycle (Oikawa et al.
427 2010). RANK-ligand (RANKL) expressed by osteoblasts activates pre-osteoclasts to become
428 mature osteoclasts through binding to receptor activator of nuclear factor- κ B (RANK) receptors
429 (Poole et al. 2005; Wijenayaka et al. 2011). Sclerostin, released by osteocytes in response to
430 mechanical forces, has been reported to increase in diabetes (Hie et al. 2007; Kim et al. 2015).
431 Sclerostin inhibits osteoblast differentiation and bone formation by antagonizing the canonical
432 Wnt pathway. It also upregulates RANKL and downregulates OPG, leading to increased
433 osteoclast activity and bone resorption. Our study showed that irisin treatment significantly
434 decreased sclerostin levels in both normal and diabetic samples as shown in earlier studies
435 (Colaianni et al. 2015; Klangjareonchai et al. 2014; Zhang et al. 2018). Sclerostin inhibits
436 osteoblast differentiation and bone formation by antagonizing the canonical Wnt pathway
437 (Delgado-Calle et al. 2017). It also upregulates RANKL and downregulates OPG, leading to
438 increased osteoclast activity and bone resorption (Poole et al. 2005). In osteoclasts, the
439 expression of cathepsin K, TRAP (tartrate-resistant acid phosphatase), and carbonic anhydrase-2
440 proteins, involved in the remodeling of the extracellular matrix are upregulated by sclerostin
441 (Wijenayaka et al. 2011).

442 The osteoblastic activity was estimated by measuring the osteocalcin levels in serum and bone
443 samples. Our study also found that untreated diabetic samples had reduced osteocalcin levels,
444 indicating decreased osteoblastic activity. Treatment with irisin showed anabolic effects,
445 although not statistically significant, by increasing osteocalcin release. Suppression of sclerostin
446 in treated samples likely contributed to improved bone formation. The data obtained from this
447 study is consistent with others which also demonstrated decreased bone formation in diabetes by
448 the significantly decreased level of osteocalcin (Horcajada-Molteni et al. 2001; Li et al. 2005).
449 Hyperglycemia in diabetes inhibits osteoblast proliferation, promotes osteoclast differentiation,
450 decreases osteocalcin and OPG expression, and reduces bone mineral density. Irisin directly acts
451 on osteoblasts, stimulating proliferation and differentiation through the p38 MAPK and ERK
452 pathways (Qiao et al. 2016).
453 Bone resorption was investigated in this study by measuring carboxy-terminal collagen
454 crosslinks (CTX-1) levels in bone and serum samples and consistent with other studies, (Khan &
455 Fraser 2015; Qiao et al. 2016) it was found that bone resorption significantly increases in DM.
456 Further, irisin treatment did not significantly affect the osteoclastic activity in the diabetic
457 samples possibly due to the limited number of samples. A significant change was, however,
458 recorded in the bones of normal rats as irisin treatment further increases the osteoclastic activity
459 as shown by (Ng et al. 2018). Irisin was shown in an earlier study to induce osteoclastogenesis by
460 acting on integrin which, subsequently acts as the receptor for irisin on osteoclasts. Irisin-
461 induced osteoclastogenesis led to the release of carboxy-terminal collagen crosslinks (CTX) and
462 enhanced bone resorption (Kim et al. 2018).
463 To our knowledge, this is the first study to report the positive effect of irisin on the trabecular
464 bone microstructure in DM1. Irisin treatment significantly improves the Tb. N and improves Tb.
465 Sp, BV/TV, and BMD by 22%-28%. The small change could be attributed to a very low dose of
466 irisin and the small number of animals used in this pilot study. However, the study also found
467 that low doses of irisin significantly decreased sclerostin, an anti-anabolic osteokine in diabetic
468 osteopathy.

469
470

471 **Conclusions**

472 The data obtained using a micro-CT analysis corroborates that DM deteriorates the trabecular
473 bone microstructure in the proximal end of the femur which is only partially improved by irisin.
474 Bone formation is adversely affected in STZ-induced diabetic osteopathy which is shown in this
475 study by decreased osteocalcin and increased CTX1 and sclerostin levels. Irisin is a regulator of
476 bone remodeling by acting on all the key players of the bone remodeling cycle. Irisin
477 significantly decreases sclerostin levels in diabetic rats which most likely promotes osteoblast
478 differentiation and bone formation enhancing the trabecular bone quality. However, regarding
479 trabecular bone parameters, statistically significant improvement with the irisin treatment is
480 observed only in the trabecular number. Bone mineral density, bone volume fraction, and
481 trabecular separation improved by 22%-28% only and this could be due to the small sample size

482 and a small dose of irisin used for this pilot study. Conversely, irisin also promotes osteoclastic
483 activity, therefore, would help to treat diabetic osteopathy where low bone turnover is the
484 underlying pathology. However, the changes reported here with irisin treatment were marginal
485 and further work with variable doses of irisin is required to establish the role of irisin in diabetic
486 osteopathy.

487 **Acknowledgments**

488 We are grateful to the members of the animal house facility and Ms. Crystal D'souza and Ms. Sara Saeed
489 Dewaib Rahmah Alhmoudi for animal handling at the College of Medicine and Health Sciences, United
490 Arab Emirates University, UAE, Al Ain.

491

492 **Conflict of interest**

493 The authors declare no potentials conflicts of interest

494

495

496

497

498 **References**

- 499 Armas LA, Akhter MP, Drincic A, and Recker RR. 2012. Trabecular bone histomorphometry in
500 humans with Type 1 Diabetes Mellitus. *Bone* 50:91-96. 10.1016/j.bone.2011.09.055
- 501 Benedetti MG, Furlini G, Zati A, and Letizia Mauro G. 2018. The Effectiveness of Physical
502 Exercise on Bone Density in Osteoporotic Patients. *Biomed Res Int* 2018:4840531.
503 10.1155/2018/4840531
- 504 Boström P, Wu J, Jedrychowski MP, Korde A, Ye L, Lo JC, Rasbach KA, Boström EA, Choi JH,
505 Long JZ, Kajimura S, Zingaretti MC, Vind BF, Tu H, Cinti S, Højlund K, Gygi SP, and
506 Spiegelman BM. 2012. A PGC1- α -dependent myokine that drives brown-fat-like
507 development of white fat and thermogenesis. *Nature* 481:463-468. 10.1038/nature10777
- 508 Boutroy S, Vilayphiou N, Roux JP, Delmas PD, Blain H, Chapurlat RD, and Chavassieux P.
509 2011. Comparison of 2D and 3D bone microarchitecture evaluation at the femoral neck,
510 among postmenopausal women with hip fracture or hip osteoarthritis. *Bone* 49:1055-
511 1061. 10.1016/j.bone.2011.07.037
- 512 Bouxsein ML, Boyd SK, Christiansen BA, Guldborg RE, Jepsen KJ, and Muller R. 2010a.
513 Guidelines for assessment of bone microstructure in rodents using micro-computed
514 tomography. *J Bone Miner Res* 25:1468-1486. 10.1002/jbmr.141
- 515 Bouxsein ML, Boyd SK, Christiansen BA, Guldborg RE, Jepsen KJ, and Müller R. 2010b.
516 Guidelines for assessment of bone microstructure in rodents using micro-computed
517 tomography. *J Bone Miner Res* 25:1468-1486. 10.1002/jbmr.141
- 518 Cariatì I, Bonanni R, Rinaldi AM, Marini M, Iundusi R, Gasbarra E, Tancredi V and Tarantino U
519 2023. Recombinant irisin prevents cell death and mineralization defects induced by
520 random positioning machine exposure in primary cultures of human osteoblasts: A
521 promising strategy for the osteoporosis treatment. *Front. Physiol.* 14:1107933. doi:
522 10.3389/fphys.2023.1107933

- 523 Chen H, Shoumura S, Emura S, and Bunai Y. 2008. Regional variations of vertebral trabecular
524 bone microstructure with age and gender. *Osteoporos Int* 19:1473-1483.
525 10.1007/s00198-008-0593-3
- 526 Chen S, Liu D, He S, Yang L, Bao Q, Qin H, Liu H, Zhao Y, and Zong Z. 2018. Differential
527 effects of type 1 diabetes mellitus and subsequent osteoblastic β -catenin activation on
528 trabecular and cortical bone in a mouse model. *Exp Mol Med* 50:1-14. 10.1038/s12276-
529 018-0186-y
- 530 Ciarelli TE, Fyhrie DP, Schaffler MB, and Goldstein SA. 2000. Variations in three-dimensional
531 cancellous bone architecture of the proximal femur in female hip fractures and in
532 controls. *J Bone Miner Res* 15:32-40. 10.1359/jbmr.2000.15.1.32
- 533 Colaianni G, Cuscito C, Mongelli T, Pignataro P, Buccoliero C, Liu P, Lu P, Sartini L, Di Comite
534 M, Mori G, Di Benedetto A, Brunetti G, Yuen T, Sun L, Reseland JE, Colucci S, New MI,
535 Zaidi M, Cinti S, and Grano M. 2015. The myokine irisin increases cortical bone mass.
536 *Proc Natl Acad Sci U S A* 112:12157-12162. 10.1073/pnas.1516622112
- 537 Colaianni G, Mongelli T, Cuscito C, Pignataro P, Lippo L, Spiro G, Notarnicola A, Severi I,
538 Passeri G, Mori G, Brunetti G, Moretti B, Tarantino U, Colucci SC, Reseland JE, Vettor
539 R, Cinti S, and Grano M. 2017. Irisin prevents and restores bone loss and muscle
540 atrophy in hind-limb suspended mice. *Sci Rep* 7:2811. 10.1038/s41598-017-02557-8
- 541 Colberg SR, Sigal RJ, Yardley JE, Riddell MC, Dunstan DW, Dempsey PC, Horton ES,
542 Castorino K, and Tate DF. 2016. Physical Activity/Exercise and Diabetes: A Position
543 Statement of the American Diabetes Association. *Diabetes Care* 39:2065-2079.
544 10.2337/dc16-1728
- 545 Courtney AC, Wachtel EF, Myers ER, and Hayes WC. 1995. Age-related reductions in the
546 strength of the femur tested in a fall-loading configuration. *J Bone Joint Surg Am* 77:387-
547 395. 10.2106/00004623-199503000-00008
- 548 Delgado-Calle J, Sato AY, and Bellido T. 2017. Role and mechanism of action of sclerostin in
549 bone. *Bone* 96:29-37. 10.1016/j.bone.2016.10.007
- 550 Estell EG, Le PT, Vegting Y, Kim H, Wrann C, Bouxsein ML, Nagano K, Baron R, Spiegelman
551 BM, and Rosen CJ. 2020. Irisin directly stimulates osteoclastogenesis and bone
552 resorption in vitro and in vivo. *Elife* 9. 10.7554/eLife.58172
- 553 Faienza MF, Brunetti G, Sanesi L, Colaianni G, Celi M, Piacente L, D'Amato G, Schipani E,
554 Colucci S, and Grano M. 2018. High irisin levels are associated with better glycemic
555 control and bone health in children with Type 1 diabetes. *Diabetes Res Clin Pract*
556 141:10-17. 10.1016/j.diabres.2018.03.046
- 557 Formigari GP, Dátilo MN, Vareda B, Cavaglieri CR, Lopes de Faria JM, Lopes de Faria JB.
558 2022. Renal protection induced by physical exercise may be mediated by the irisin/AMPK
559 axis in diabetic nephropathy. *Sci Rep* 12, 9062 <https://doi.org/10.1038/s41598-022-13054-y>
- 560
- 561 Furman BL. 2015. Streptozotocin-Induced Diabetic Models in Mice and Rats. *Curr Protoc*
562 *Pharmacol* 70:5.47.41-45.47.20. 10.1002/0471141755.ph0547s70
- 563 Gallacher SJ, Fenner JA, Fisher BM, Quin JD, Fraser WD, Logue FC, Cowan RA, Boyle IT, and
564 MacCuish AC. 1993. An evaluation of bone density and turnover in premenopausal
565 women with type 1 diabetes mellitus. *Diabet Med* 10:129-133. 10.1111/j.1464-
566 5491.1993.tb00029.x
- 567 Greenwood C, Clement J, Dicken A, Evans P, Lyburn I, Martin RM, Stone N, Zioupos P, and
568 Rogers K. 2018. Age-Related Changes in Femoral Head Trabecular Microarchitecture.
569 *Aging Dis* 9:976-987. 10.14336/AD.2018.0124
- 570 Hie M, Shimono M, Fujii K, and Tsukamoto I. 2007. Increased cathepsin K and tartrate-resistant
571 acid phosphatase expression in bone of streptozotocin-induced diabetic rats. *Bone*
572 41:1045-1050. 10.1016/j.bone.2007.08.030

- 573 Holmes D. 2015. Bone: Irisin boosts bone mass. *Nat Rev Endocrinol* 11:689.
574 10.1038/nrendo.2015.174
- 575 Horcajada-Molteni MN, Chanteranne B, Lebecque P, Davicco MJ, Coxam V, Young A, and
576 Barlet JP. 2001. Amylin and bone metabolism in streptozotocin-induced diabetic rats. *J*
577 *Bone Miner Res* 16:958-965. 10.1359/jbmr.2001.16.5.958
- 578 Hough FS, Pierroz DD, Cooper C, Ferrari SL, and Group ICBaDW. 2016. MECHANISMS IN
579 ENDOCRINOLOGY: Mechanisms and evaluation of bone fragility in type 1 diabetes
580 mellitus. *Eur J Endocrinol* 174:R127-138. 10.1530/EJE-15-0820
- 581 Hygum K, Starup-Linde J, and Langdahl BL. 2019. Diabetes and bone. *Osteoporos Sarcopenia*
582 5:29-37. 10.1016/j.afos.2019.05.001
- 583 Janghorbani M, Feskanich D, Willett WC, and Hu F. 2006. Prospective study of diabetes and
584 risk of hip fracture: the Nurses' Health Study. *Diabetes Care* 29:1573-1578.
585 10.2337/dc06-0440
- 586 Janghorbani M, Van Dam RM, Willett WC, and Hu FB. 2007. Systematic review of type 1 and
587 type 2 diabetes mellitus and risk of fracture. *Am J Epidemiol* 166:495-505.
588 10.1093/aje/kwm106
- 589 Kelly NH, Schimenti JC, Patrick Ross F, and van der Meulen MC. 2014. A method for isolating
590 high quality RNA from mouse cortical and cancellous bone. *Bone* 68:1-5.
591 10.1016/j.bone.2014.07.022
- 592 Khan TS, and Fraser LA. 2015. Type 1 diabetes and osteoporosis: from molecular pathways to
593 bone phenotype. *J Osteoporos* 2015:174186. 10.1155/2015/174186
- 594 Kim JH, Lee DE, Woo GH, Cha JH, Bak EJ, and Yoo YJ. 2015. Osteocytic Sclerostin
595 Expression in Alveolar Bone in Rats With Diabetes Mellitus and Ligature-Induced
596 Periodontitis. *J Periodontol* 86:1005-1011. 10.1902/jop.2015.150083
- 597 Kim H, Wrann CD, Jedrychowski M, Vidoni S, Kitase Y, Nagano K, Zhou C, Chou J, Parkman
598 VA, Novick SJ, Strutzenberg TS, Pascal BD, Le PT, Brooks DJ, Roche AM, Gerber KK,
599 Mattheis L, Chen W, Tu H, Bouxsein ML, Griffin PR, Baron R, Rosen CJ, Bonewald LF,
600 and Spiegelman BM. 2018. Irisin Mediates Effects on Bone and Fat via α V Integrin
601 Receptors. *Cell* 175:1756-1768.e1717. 10.1016/j.cell.2018.10.025
- 602 Klangjareonchai T, Nimitphong H, Saetung S, Bhirommuang N, Samittarucksak R,
603 Chanprasertyothin S, Sudatip R, and Ongphiphadhanakul B. 2014. Circulating sclerostin
604 and irisin are related and interact with gender to influence adiposity in adults with
605 prediabetes. *Int J Endocrinol* 2014:261545. 10.1155/2014/261545
- 606 Kutlu E, Ozgen LT, Bulut H, Kocyigit A, Ustunova S, Hüseyinbas O, Torun E, Cesur Y. 2023.
607 Investigation of irisin's role in pubertal onset physiology in female rats. *Peptides*
608 163:170976. doi: 10.1016/j.2023.170976
- 609 Lebiecz-Odrobina D, and Kay J. 2010.
610 Rheumatic manifestations of diabetes mellitus. *Rheum Dis Clin North Am* 36:681-699.
611 10.1016/j.rdc.2010.09.008
- 612 Legrand E, Chappard D, Pascaretti C, Duquenne M, Krebs S, Rohmer V, Basle MF, and Audran
613 M. 2000. Trabecular bone microarchitecture, bone mineral density, and vertebral
614 fractures in male osteoporosis. *J Bone Miner Res* 15:13-19. 10.1359/jbmr.2000.15.1.13
- 615 Lelovas PP, Xanthos TT, Thoma SE, Lyritis GP, Dontas IA.(2008) The laboratory rat as an
616 animal model for osteoporosis research. *Comp Med* 58(5):424-30. PMID: 19004367;
PMCID: PMC2707131.
- 617 Li X, Zhang Y, Kang H, Liu W, Liu P, Zhang J, Harris SE, and Wu D. 2005. Sclerostin binds to
618 LRP5/6 and antagonizes canonical Wnt signaling. *J Biol Chem* 280:19883-19887.
619 10.1074/jbc.M413274200
- 620 Liu S, Du F, Li X, Wang M, Duan R, Zhang J, Wu Y, and Zhang Q. 2017. Effects and underlying
621 mechanisms of irisin on the proliferation and apoptosis of pancreatic β cells. *PLoS One*
622 12:e0175498. 10.1371/journal.pone.0175498

- 623 Ma Y, Qiao X, Zeng R, Cheng R, Zhang J, Luo Y, Nie Y, Hu Y, Yang Z, Liu L, Xu W, Xu CC,
624 and Xu L. 2018. Irisin promotes proliferation but inhibits differentiation in osteoclast
625 precursor cells. *FASEB J*:fj201700983RR. 10.1096/fj.201700983RR
- 626 Maggio AB, Ferrari S, Kraenzlin M, Marchand LM, Schwitzgebel V, Beghetti M, Rizzoli R, and
627 Farpour-Lambert NJ. 2010. Decreased bone turnover in children and adolescents with
628 well controlled type 1 diabetes. *J Pediatr Endocrinol Metab* 23:697-707.
629 10.1515/jpem.2010.23.7.697
- 630 Mahgoub MO, D'Souza C, Al Darmaki RSMH, Baniyas MMYH, and Adeghate E. 2018. An
631 update on the role of irisin in the regulation of endocrine and metabolic functions.
632 *Peptides* 104:15-23. 10.1016/j.peptides.2018.03.018
- 633 Marshall D, Johnell O, and Wedel H. 1996. Meta-analysis of how well measures of bone mineral
634 density predict occurrence of osteoporotic fractures. *BMJ* 312:1254-1259.
635 10.1136/bmj.312.7041.1254
- 636 Mazur-Bialy AI, Pocheć E, and Zarawski M. 2017. Anti-Inflammatory Properties of Irisin,
637 Mediator of Physical Activity, Are Connected with TLR4/MyD88 Signaling Pathway
638 Activation. *Int J Mol Sci* 18. 10.3390/ijms18040701
- 639 McCalden RW, McGeough JA, and Court-Brown CM. 1997. Age-related changes in the
640 compressive strength of cancellous bone. The relative importance of changes in density
641 and trabecular architecture. *J Bone Joint Surg Am* 79:421-427. 10.2106/00004623-
642 199703000-00016
- 643 Milovanovic P, Djonic D, Marshall RP, Hahn M, Nikolic S, Zivkovic V, Amling M, and Djuric M.
644 2012. Micro-structural basis for particular vulnerability of the superolateral neck
645 trabecular bone in the postmenopausal women with hip fractures. *Bone* 50:63-68.
646 10.1016/j.bone.2011.09.044
- 647 Miyake H, Kanazawa I, and Sugimoto T. 2018. Association of Bone Mineral Density, Bone
648 Turnover Markers, and Vertebral Fractures with All-Cause Mortality in Type 2 Diabetes
649 Mellitus. *Calcif Tissue Int* 102:1-13. 10.1007/s00223-017-0324-x
- 650 Mohsin S, Kaimala S, AlTamimi EKY, Tariq S, and Adeghate E. 2019a. In vivo Labeling of Bone
651 Microdamage in an Animal Model of Type 1 Diabetes Mellitus. *Sci Rep* 9:16994.
652 10.1038/s41598-019-53487-6
- 653 Mohsin S, Kaimala S, Sunny JJ, Adeghate E, and Brown EM. 2019b. Type 2 Diabetes Mellitus
654 Increases the Risk to Hip Fracture in Postmenopausal Osteoporosis by Deteriorating the
655 Trabecular Bone Microarchitecture and Bone Mass. *J Diabetes Res* 2019:3876957.
656 10.1155/2019/3876957
- 657 Motyl K, and McCabe LR. 2009. Streptozotocin, type I diabetes severity and bone. *Biol Proced*
658 *Online* 11:296-315. 10.1007/s12575-009-9000-5
- 659 Motyl KJ, Botolin S, Irwin R, Appledorn DM, Kadakia T, Amalfitano A, Schwartz RC, and
660 McCabe LR. 2009. Bone inflammation and altered gene expression with type I diabetes
661 early onset. *J Cell Physiol* 218:575-583. 10.1002/jcp.21626
- 662 Napoli N, Chandran M, Pierroz DD, Abrahamsen B, Schwartz AV, Ferrari SL, and Group
663 IBAW. 2017. Mechanisms of diabetes mellitus-induced bone fragility. *Nat Rev*
664 *Endocrinol* 13:208-219. 10.1038/nrendo.2016.153
- 665 Ng AY, Tu C, Shen S, Xu D, Oursler MJ, Qu J, and Yang S. 2018. Comparative
666 Characterization of Osteoclasts Derived From Murine Bone Marrow Macrophages and
667 RAW 264.7 Cells Using Quantitative Proteomics. *JBMR Plus* 2:328-340.
668 10.1002/jbm4.10058
- 669 Oikawa A, Siragusa M, Quaini F, Mangialardi G, Katare RG, Caporali A, van Buul JD, van
670 Alphen FP, Graiani G, Spinetti G, Kraenkel N, Prezioso L, Emanuelli C, and Madeddu P.
671 2010. Diabetes mellitus induces bone marrow microangiopathy. *Arterioscler Thromb*
672 *Vasc Biol* 30:498-508. 10.1161/ATVBAHA.109.200154

- 673 Poole KE, van Bezooijen RL, Loveridge N, Hamersma H, Papapoulos SE, Löwik CW, and
674 Reeve J. 2005. Sclerostin is a delayed secreted product of osteocytes that inhibits bone
675 formation. *FASEB J* 19:1842-1844. 10.1096/fj.05-4221fje
- 676 Qiao X, Nie Y, Ma Y, Chen Y, Cheng R, Yin W, Hu Y, Xu W, and Xu L. 2016. Irisin promotes
677 osteoblast proliferation and differentiation via activating the MAP kinase signaling
678 pathways. *Sci Rep* 6:18732. 10.1038/srep18732
- 679 Rana KS, Pararasa C, Afzal I, Nagel DA, Hill EJ, Bailey CJ, Griffiths HR, Kyrou I, Randeva HS,
680 Bellary S, and Brown JE. 2017. Plasma irisin is elevated in type 2 diabetes and is
681 associated with increased E-selectin levels. *Cardiovasc Diabetol* 16:147.
682 10.1186/s12933-017-0627-2
- 683 Riggs BL, and Parfitt AM. 2005. Drugs used to treat osteoporosis: the critical need for a uniform
684 nomenclature based on their action on bone remodeling. *J Bone Miner Res* 20:177-184.
685 10.1359/JBMR.041114
- 686 Saito M, Fujii K, Mori Y, and Marumo K. 2006. Role of collagen enzymatic and glycation induced
687 cross-links as a determinant of bone quality in spontaneously diabetic WBN/Kob rats.
688 *Osteoporos Int* 17:1514-1523. 10.1007/s00198-006-0155-5
- 689 Shah VN, Sippl R, Joshee P, Pyle L, Kohrt WM, Schauer IE, and Snell-Bergeon JK. 2018.
690 Trabecular bone quality is lower in adults with type 1 diabetes and is negatively
691 associated with insulin resistance. *Osteoporos Int* 29:733-739. 10.1007/s00198-017-
692 4353-0
- 693 Siris ES, Miller PD, Barrett-Connor E, Faulkner KG, Wehren LE, Abbott TA, Berger ML, Santora
694 AC, and Sherwood LM. 2001. Identification and fracture outcomes of undiagnosed low
695 bone mineral density in postmenopausal women: results from the National Osteoporosis
696 Risk Assessment. *JAMA* 286:2815-2822. 10.1001/jama.286.22.2815
- 697 Tentolouris A, Eleftheriadou I, Tsilingiris D, Anastasiou IA, Kosta OA, Mourouzis I, Kokkinos A,
698 Pantos C, Katsilambros N, and Tentolouris N. 2018. Plasma Irisin Levels in Subjects
699 with Type 1 Diabetes: Comparison with Healthy Controls. *Horm Metab Res* 50:803-810.
700 10.1055/a-0748-6170
- 701 Thomsen JS, Ebbesen EN, and Mosekilde L. 1998. Relationships between static
702 histomorphometry and bone strength measurements in human iliac crest bone biopsies.
703 *Bone* 22:153-163. 10.1016/s8756-3282(97)00235-4
- 704 Thomsen JS, Ebbesen EN, and Mosekilde LI. 2002. Age-related differences between thinning of
705 horizontal and vertical trabeculae in human lumbar bone as assessed by a new
706 computerized method. *Bone* 31:136-142. 10.1016/s8756-3282(02)00801-3
- 707 Vestergaard P. 2007. Discrepancies in bone mineral density and fracture risk in patients with
708 type 1 and type 2 diabetes--a meta-analysis. *Osteoporos Int* 18:427-444.
709 10.1007/s00198-006-0253-4
- 710 Wijenayaka AR, Kogawa M, Lim HP, Bonewald LF, Findlay DM, and Atkins GJ. 2011. Sclerostin
711 stimulates osteocyte support of osteoclast activity by a RANKL-dependent pathway.
712 *PLoS One* 6:e25900. 10.1371/journal.pone.0025900
- 713 Zhang D, Bae C, Lee J, Jin Z, Kang M, Cho YS, Kim JH, Lee W, and Lim SK. 2018. The bone
714 anabolic effects of irisin are through preferential stimulation of aerobic glycolysis. *Bone*
715 114:150-160. 10.1016/j.bone.2018.05.013
- 716 Zhang ZM, Li ZC, Jiang LS, Jiang SD, and Dai LY. 2010. Micro-CT and mechanical evaluation
717 of subchondral trabecular bone structure between postmenopausal women with
718 osteoarthritis and osteoporosis. *Osteoporos Int* 21:1383-1390. 10.1007/s00198-009-
719 1071-2
- 720

Figure 1

A streptozotocin-induced rat model of type 1 diabetic osteopathy injected with a low dose of irisin.

Figure Prepared using Canva software

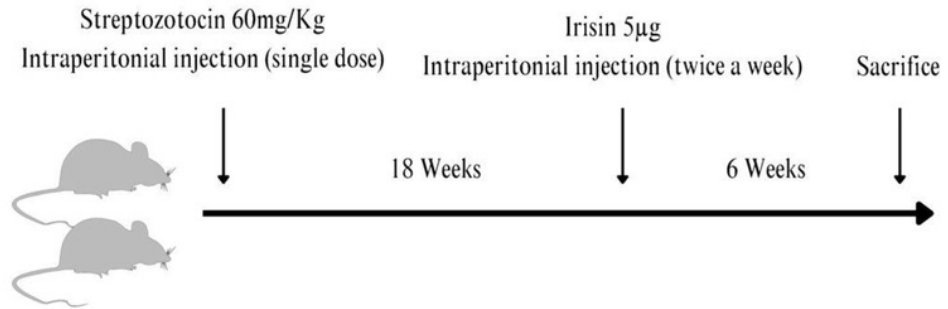


Figure 2

Representation of 3D microarchitecture of the trabecular bone obtained by using the micro-CT. Plots of changes in various structural parameters of trabecular bone in all experimental groups is shown.

Representation of 3D microarchitecture of the trabecular bone at the proximal end of the femur is shown in frontal (A, C, E, and G) and cross-sectional (B, D, F, and H) images from four groups: A and B (Normal un-treated/ NUT), C & D (Normal treated / NT), E and F (diabetic un-treated / DMUT), and G & H (treated / DMT) obtained by using the micro-CT. The image I is the magnified image of (A) to show the region of interest for frontal (red box) and cross-sectional (blue line) images. Plots of changes in various structural parameters of trabecular bone n=3/Gp: (J) Trabecular separation (Tb-Sp) (K) Trabecular thickness (Tb-Th) (L) Trabecular number (Tb-N) (M) Bone volume/total volume BV/TV, (N) Bone surface density (BS/TV) (O) mean 1 (BMD), from NUT, NT, DMUT, DMT compared. P values are indicated in brackets.

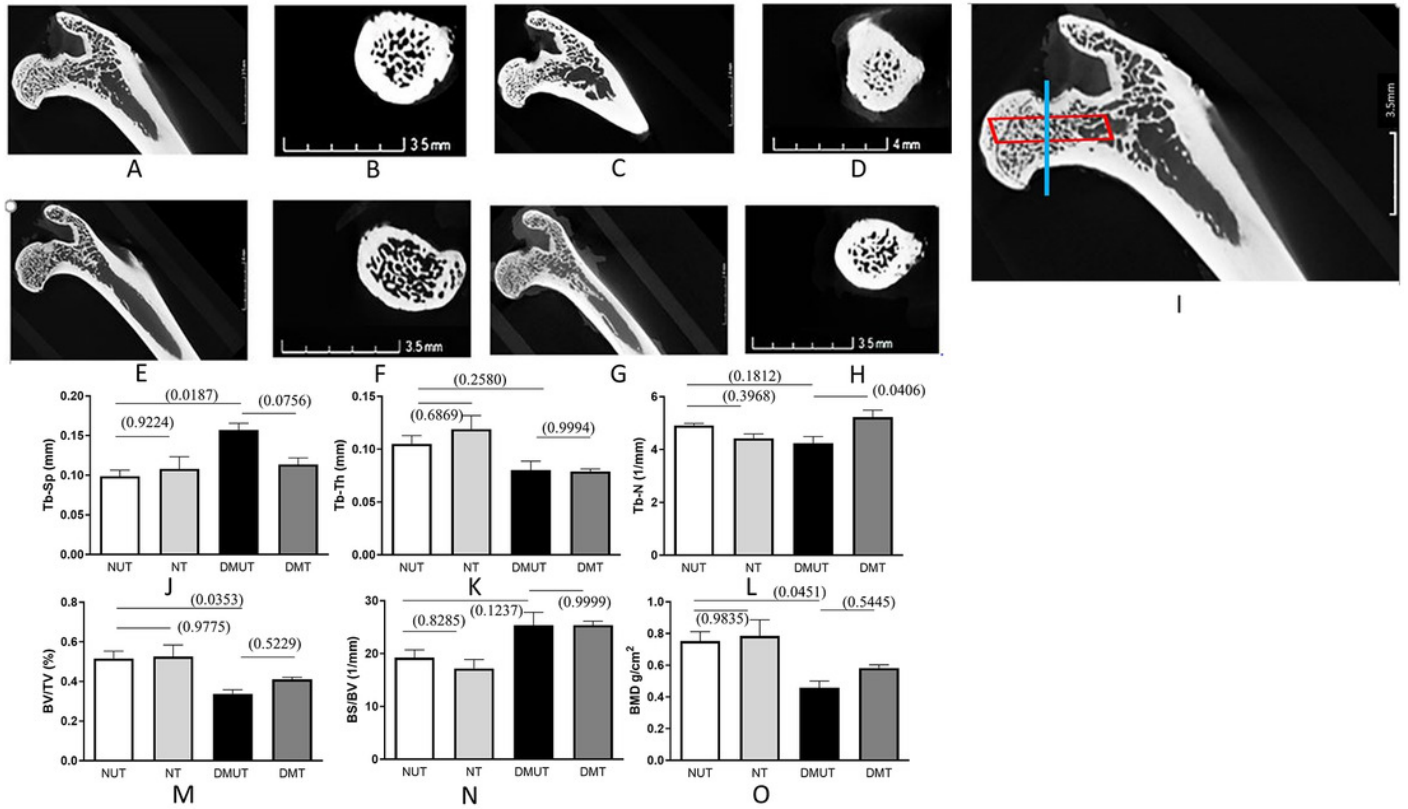


Figure 3

Plots of changes in bone markers in sera and bone tissue

Plots of changes in bone markers in sera and bone tissue is shown (A-E) in all four groups (Normal un-treated NUT: Normal Treated NT: Diabetic untreated DMUT: Diabetic treated DMT) n= 3-5/Gp; F (n=3-4/Gp): (A) Serum osteocalcin (ng/ml) (B) Bone osteocalcin (pg/ml) (C) Serum CTX1 (ng/ml)(D) Bone CTX1 (pg/ml). Relative SOST expression is shown by PCR (E), Western blot (F). P values are indicated in brackets. Error bars = Mean \pm SE.

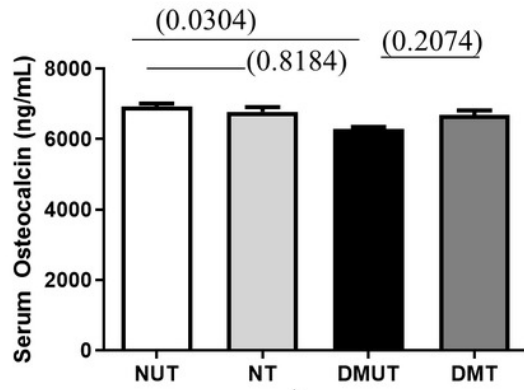
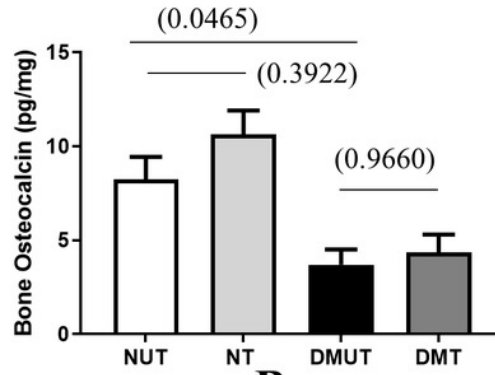
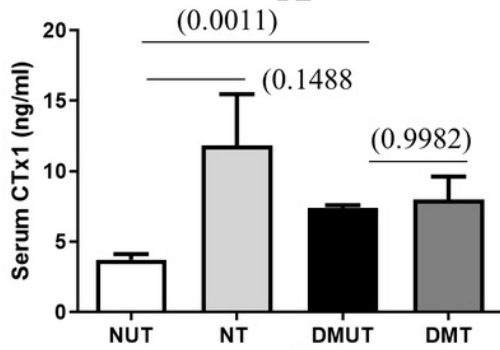
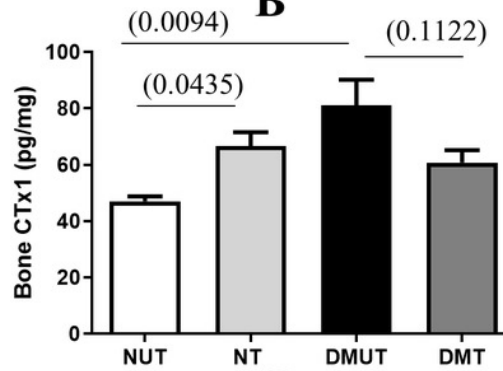
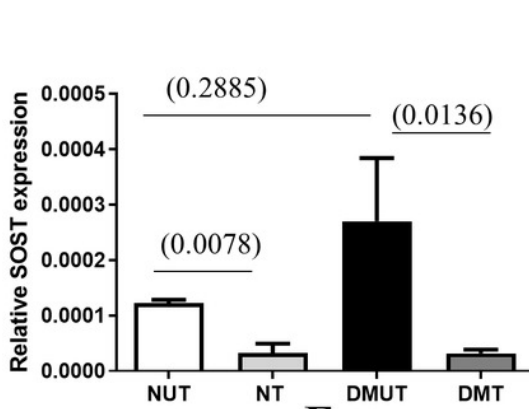
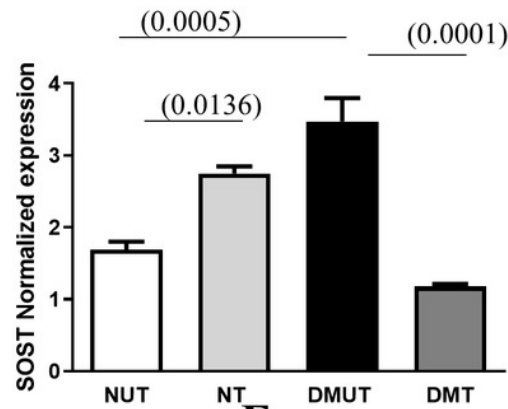
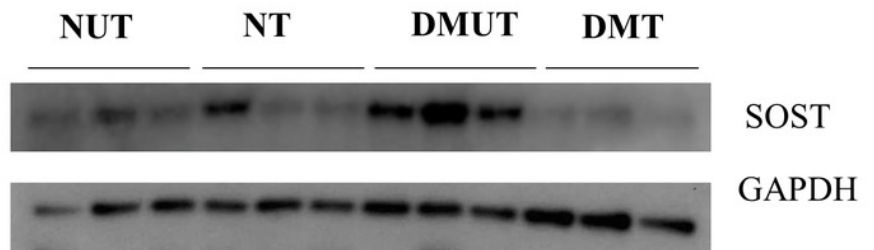
**A****B****C****D****E****F**

Table 1 (on next page)

Mean \pm S.E between different groups related to trabecular bone parameters

Mean \pm S.E between different groups related to trabecular bone parameters obtained using micro-CT. Gp. I—normal un-treated/ NUT, Gp. II— normally treated (NT), Gp. III—diabetic un-treated (DMUT), and Gp. IV—diabetic treated (DMT). Trabecular separation Tb-Sp Gp (I-III = $P < 0.05$): Trabecular thickness Tb-Th Gp (II-III; II-IV = $P < 0.05$): Trabecular number Tb-N Gp (III-IV = $P < 0.05$): bone volume/total volume BV/TV Gp (I-III; II-III = $P < 0.05$): bone surface density BS/ BV Gp (II-III; II-IV $P < 0.05$): Bone mineral density BMD Gp (I-III; II-III = $P < 0.05$). $n=3$ /Gp.

Parameters	Mean \pm S.E in the experimental Groups			
	NUT	NT	DMUT	DMT
Tb-Sp (mm)	0.09867 \pm 0.007781	0.1079 \pm 0.01554 * with DMUT	0.1570 \pm 0.008653 * with NUT	0.1137 \pm 0.008182
Tb-Th (mm)	0.1051 \pm 0.007647	0.1189 \pm 0.01297	0.0803 \pm 0.008294 * with NT	0.0789 \pm 0.002389 * with NT
Tb-N (1/mm)	4.910 \pm 0.08251	4.422 \pm 0.1725	4.243 \pm 0.2492	5.222 \pm 0.2683 * with DMUT
BV/TV %	0.5159 \pm 0.03683	0.5255 \pm 0.05855 * with DMUT	0.3376 \pm 0.02096 * with NUT	0.4109 \pm 0.01061
BS/BV 1/mm	19.24 \pm 1.478	17.19 \pm 1.704	25.39 \pm 2.427 * with NT	25.39 \pm 0.7572 * with NT
BMD g/cm²	0.7527 \pm 0.05921	0.7847 \pm 0.1022 * with NUT	0.4580 \pm 0.04238 * with NUT	0.5820 \pm 0.02126

- 1 ○ *= p<0.05
- 2 ○ Normal untreated NUT (Control+vehicle)
- 3 ○ Normal treated NT (Control+irisin)
- 4 ○ Diabetic untreated DMUT (Diabetic+vehicle)
- 5 ○ Gp IV Diabetic treated DMT Diabetic+irisin

6

7

8